

# Synthesis, Structure, and Thermophysical Properties of an Energetic Complex $\text{Co}(3\text{-(2-pyridyl)-5-(3'-pyridyl)-1H-1,2,4-triazole})_3 \cdot \text{H}_2\text{O}$

Bing Li, Qing Wei, Qi Yang, Sanping Chen,\* and Shengli Gao\*

Key Laboratory of Synthetic and Natural Functional Molecule Chemistry of Ministry of Education, College of Chemistry and Materials Science, Northwest University, Xi'an 710069, P. R. China

**S** Supporting Information

**ABSTRACT:** A new energetic complex,  $\text{Co}(2,3'\text{-bpt})_3 \cdot \text{H}_2\text{O}$  (**1**) ( $2,3'\text{-Hbpt} = 3\text{-(2-pyridyl)-5-(3'-pyridyl)-1H-1,2,4-triazole}$ ), was synthesized and characterized by single crystal X-ray diffraction method. Crystallographic data are as follows: triclinic,  $P\bar{1}$  space group,  $a = 10.323(2)$  Å,  $b = 11.261(2)$  Å,  $c = 16.139(3)$  Å,  $\alpha = 89.022(3)^\circ$ ,  $\beta = 71.794(2)^\circ$ ,  $\gamma = 66.990(2)^\circ$ ,  $Z = 2$ . In addition, the thermal analysis of  $\text{Co}(2,3'\text{-bpt})_3 \cdot \text{H}_2\text{O}$  has been performed by thermogravimetric-differential thermogravimetric (TG-DTG) techniques. The thermal decomposition of ammonium perchlorate (AP) with complex **1** was explored by differential scanning calorimetry (DSC) over the temperature range from (323 to 773) K. AP is completely decomposed in a shorter time in the presence of complex **1**, and the decomposition heat of the mixture is  $2.034 \text{ kJ} \cdot \text{g}^{-1}$ , significantly higher than pure AP. By Kissinger's method, the ratio of  $E_a/\ln(A)$  is 12.66 for the mixture, which indicates that complex **1** shows good catalytic activity toward AP decomposition.

## INTRODUCTION

Ammonium perchlorate (AP) is a common oxidizer in composite solid propellants, and its thermal decomposition characteristics directly influence the combustion behavior of solid propellants.<sup>1–5</sup> Many effective combustion catalysts on the thermal decomposition of AP, such as metal salts of triazole and its derivatives, have been reported.<sup>6,7</sup> As one of the derivatives of triazole, 3-(2-pyridyl)-5-(3'-pyridyl)-1H-1,2,4-triazole (2,3'-Hbpt) can serve as an  $N,N'$ -donor and act as a bridge ligand, thus mediate exchange coupling.<sup>8–10</sup> Moreover, the prototropy and conjugation among the 1H-1,2,4-triazole and pyridyl groups not only alter the electron density in different sections of the molecules but make the ligand more flexible.<sup>11–13</sup> We anticipate that the complex of Hbpt would follow the examples of nitrotriazolone (NTO) compounds<sup>14</sup> which accelerate the thermolysis of AP.

With this understanding, we report the synthesis, crystal structure, and thermal properties of  $[\text{Co}(2,3'\text{-bpt})_3] \cdot \text{H}_2\text{O}$ . The catalytic performances of complex **1** on AP decomposition are studied, which shows complex **1** can accelerate the decomposition of AP.

## EXPERIMENTAL SECTION

**Chemicals and Apparatus.** All reagents for the syntheses were purchased from Tokyo Kasei Kogyo Co., Ltd. and were of analytical reagent (A.R.) grade with a purity of 99 %.

Elemental analyses (C, H, and N) were performed on a Vario EL III analyzer. Infrared spectra drawn at regular intervals were recorded on a Bruker Fourier transform infrared (FTIR) instrument as KBr pellets. The thermogravimetric-differential thermogravimetric (TG-DTG) experiment was performed on a NETZSCH STA 449C thermal analyzer, from (323 to 1173) K with a heating rate of  $10 \text{ K} \cdot \text{min}^{-1}$  under static air atmosphere. The differential scanning calorimetry (DSC) experiment was performed on the thermal analyzer of Perkin-Elmer Pyris 6 DSC

**Table 1. Crystal Data and Structure Refinement Parameters for Complex 1**

empirical formula	$\text{C}_{36}\text{H}_{26}\text{CoN}_{15}\text{O}$
formula weight ( $\text{g} \cdot \text{mol}^{-1}$ )	743.65
crystal system	triclinic
space group	$P\bar{1}$
$a$ (Å)	10.323(2)
$b$ (Å)	11.261(2)
$c$ (Å)	16.139(3)
$\alpha$ (deg)	89.022(3)
$\beta$ (deg)	71.794(2)
$\gamma$ (deg)	66.990(2)
$Z$	2
$D_c$ ( $\text{Mg} \cdot \text{m}^{-3}$ )	1.517
$F(000)$	764
$\theta$ range for data collection (deg)	1.98 to 25.10
absorption coefficient ( $\text{mm}^{-1}$ )	0.585
$R_{\text{int}}$	0.0401
reflections collected/unique	8235/5709
final $R$ indices [ $I > 2\sigma(I)$ ]	$R_1 = 0.0650$ , $wR_2 = 0.1580$
$R$ indices (all data)	$R_1 = 0.1332$ , $wR_2 = 0.2005$
largest diff. peak and hole ( $\text{e} \cdot \text{Å}^{-3}$ )	0.309 and $-0.465$

(calibrated by standard pure indium and zinc) with a heating rate of (5, 10, 15, and 20)  $\text{K} \cdot \text{min}^{-1}$  from (323 to 773) K.

The single crystal X-ray experiment was performed on a Bruker Smart Apex charge-coupled device (CCD) diffractometer equipped with graphite monochromatized Mo  $K\alpha$  radiation

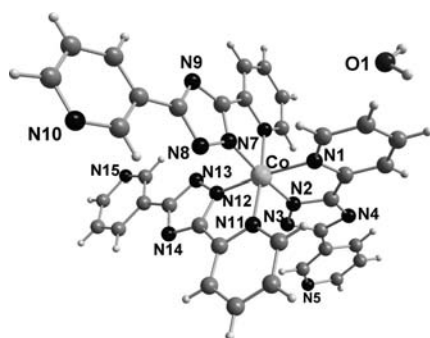
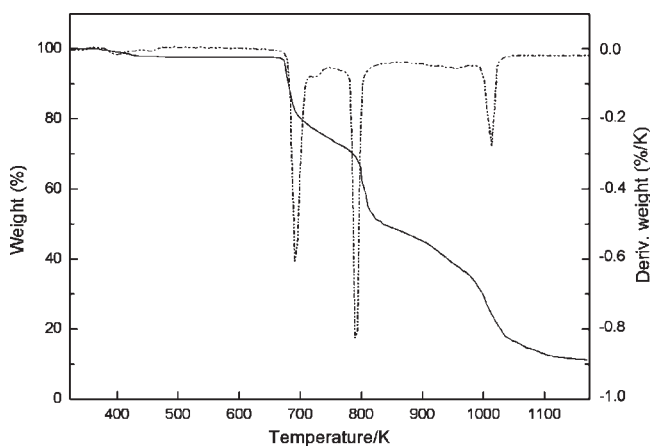
**Received:** January 24, 2011

**Accepted:** May 28, 2011

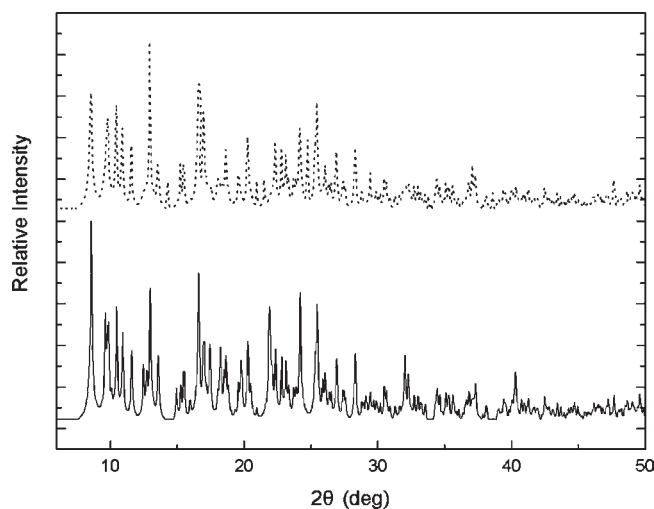
**Published:** June 08, 2011

**Table 2.** Selected Bond Lengths (Å) and Bond Angles (deg) for Complex 1

Bond Lengths			
Co(1)–N(12)	1.871(4)	Co(1)–N(11)	1.940(4)
Co(1)–N(7)	1.887(4)	Co(1)–N(6)	1.957(4)
Co(1)–N(2)	1.902(4)	Co(1)–N(1)	1.973(5)
Bond Angles			
N(12)–Co(1)–N(7)	88.63(2)	N(2)–Co(1)–N(6)	93.39(2)
N(12)–Co(1)–N(2)	93.95(2)	N(11)–Co(1)–N(6)	174.94(2)
N(7)–Co(1)–N(2)	175.25(2)	N(12)–Co(1)–N(1)	174.75(2)
N(12)–Co(1)–N(11)	82.39(2)	N(7)–Co(1)–N(1)	96.00(2)
N(7)–Co(1)–N(11)	93.89(2)	N(2)–Co(1)–N(1)	81.58(2)
N(2)–Co(1)–N(11)	90.41(2)	N(11)–Co(1)–N(1)	94.86(2)
N(12)–Co(1)–N(6)	94.00(2)	N(6)–Co(1)–N(1)	89.02(2)
N(7)–Co(1)–N(6)	82.45(2)		

**Figure 1.** Molecular structure of complex 1.**Figure 2.** TGA curves for complex 1.

( $\lambda = 0.71073 \text{ \AA}$ ) using  $\omega$  and  $\varphi$  scan mode. The single-crystal structure of complex was solved by direct methods and refined with full-matrix least-squares refinements based on  $F^2$  using SHELXS 97 and SHELXL 97.<sup>15,16</sup> All non-H atoms were located using subsequent Fourier-difference methods. In all cases hydrogen atoms were placed in calculated positions and thereafter allowed to ride on their parent atoms. Other details of crystal data, data collection parameters, and refinement statistics were given in Table 1. Selected bond distances and bond angles were given in Table 2.

**Figure 3.** Comparison of XRPD patterns of the original sample and the desolvated phases: —, original sample; ···, desolvated phases.

**Synthesis of the Complex.** 2,3'-Hbpt was synthesized according to ref 17 and further proved by IR and elemental analysis, respectively. Anal. Calcd. for  $C_{12}H_9N_5$  (%): C, 64.56; H, 4.06; N, 31.37. Found: C, 64.96; H, 4.40; N, 32.45. Mp: (528 to 529) K; IR ( $\text{cm}^{-1}$ , KBr): 3327(s), 3156(s), 3048(m), 2843(m), 1620(s), 1594(s), 1482(w), 1406(s), 1308(s), 1196(w), 1051(m), 821(m), 709(m), 625(w).

The synthesis of  $\text{Co}(2,3'\text{-bpt})_3 \cdot \text{H}_2\text{O}$  was as follows: A mixture containing  $\text{Co}(\text{OAc})_2 \cdot 2\text{H}_2\text{O}$  (21.9 mg, 0.10 mmol), 3,3'-Hbpt (11.2 mg, 0.05 mmol),  $\text{H}_2\text{O}_2$  (30 %, 0.5 mL) and water (6 mL) were sealed in a 15 mL Teflon-lined stainless steel vessel, which was heated at 413 K for 3 days and then cooled to room temperature at a rate of  $5 \text{ K} \cdot \text{h}^{-1}$ . Red prism crystals of **1** were collected in a yield of 10 % (based on Co). Anal. Calcd. for  $C_{36}H_{26}N_{15}\text{OCo}$  (%): C, 58.15; H, 3.52; N, 28.25. Found: C, 58.21; H, 3.57; N, 28.31. IR ( $\text{cm}^{-1}$ , KBr): 3396(m), 3088(m), 2643(w), 1604(s), 1550(s), 1485(s), 1461(s), 1403(s), 1378(s), 1225(m), 1038(w), 1060(w), 1020(s), 995(m), 952(w), 839(m), 771(m), 721(m), 704(s), 604(s), 508(m).

## RESULTS AND DISCUSSION

**Crystal Structure of  $\text{Co}(2,3'\text{-bpt})_3 \cdot \text{H}_2\text{O}$ .** **1** is a mononuclear complex as shown in Figure 1; the Co(III) center is in a distorted octahedral environment and coordinated by six pyridyl nitrogen atoms from three ligands. In the unit of  $[\text{Co}(2,3'\text{-bpt})_3]$ , all 2, 3'-bpt act as chelate ligands binding to the cobalt center with the Co–N distance from 1.871(4) Å to 1.973(5) Å, which was shorter than the Co–N bond of phenanthroline in chelating mode.<sup>18,19</sup> The  $\text{N} \cdots \text{Co} \cdots \text{N}$  bond angles range from  $81.58(2)^\circ$  to  $175.25(2)^\circ$ . The two pyridine ring planes in 2,3'-Hbpt ligand are slightly twisted with a dihedral angle of  $13.44^\circ$ .

**Thermal Decomposition Process of Complex .** Thermogravimetric experiments were conducted to study the thermal stability of the complex **1** (see Figure 2), which is an important parameter for metal–organic framework materials. The first weight loss with 2.57 % in the range of (370 to 461) K in the TGA curve of **1** corresponds to expulsion of the lattice water molecule (calcd. 2.42 %). The main framework remains intact until it is heated to 667 K and then releases one ligand with an exothermic peak at 697 K (found 29.80 %, calcd. 29.51 %). Then

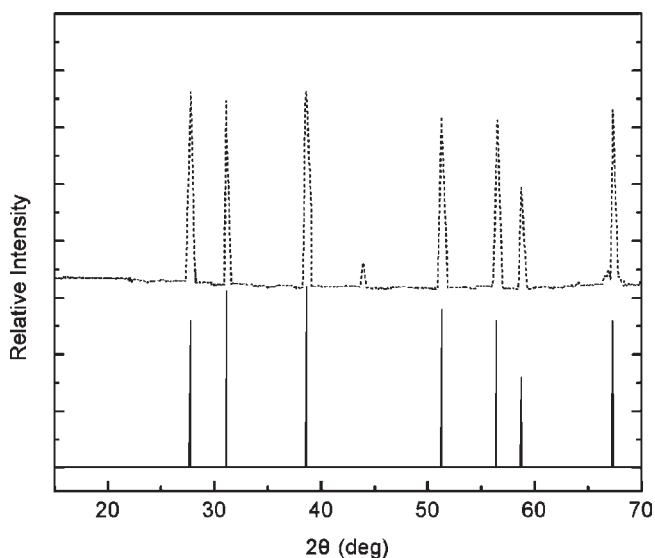


**Figure 4.** XRPD patterns of the residual: —, standard data for  $\text{Co}_2\text{O}_3$ ; ···, experimental data for the residual.

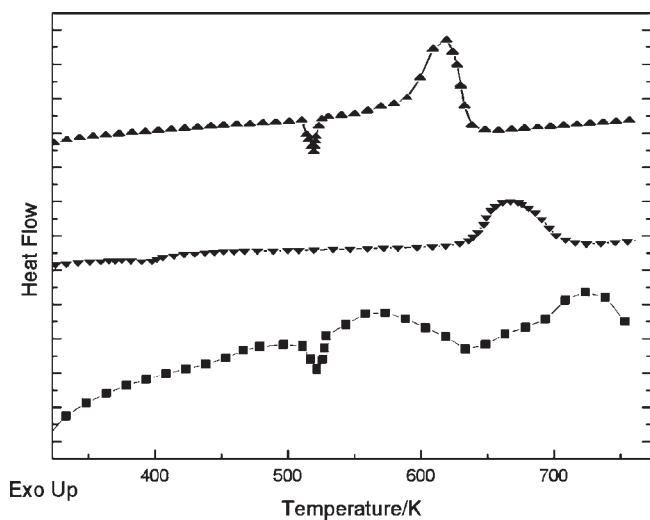


**Figure 5.** DSC curves for AP, complex 1, and AP with complex 1 at a heating rate of  $10 \text{ K} \cdot \text{min}^{-1}$ : ■, AP; ▼, complex 1; ▲, AP with complex 1.

the complex lose the other two ligands completely in the range of (798 to 1129) K with two exothermic peaks at (806 and 1022) K and convert to  $\text{Co}_2\text{O}_3$  with the residual amount of 11.26 %, which is in good agreement with the calculated value 11.19 %.

In addition, to confirm the stable framework of complex 1, the original sample and processed samples with the lattice water molecule removed were characterized by X-ray powder diffraction (XRPD) at room temperature. As shown in Figure 3, the processed samples resulted in a slightly broadened XRPD pattern with similar peak positions to that of the original sample, which shows that the crystallinity of 1 is retained. Figure 4 shows XRD patterns of the residual. It is seen that all diffraction peaks are in good agreement with the standard diffraction data for  $\text{Co}_2\text{O}_3$  (JCPDS card file No. 02-0770), while no diffractions of the impurities  $\text{CoO}$  or  $\text{Co}_3\text{O}_4$  are observed.

**Effects on Thermal Decomposition of AP.** As shown in Figure 5, the endothermic peak at 528 K for pure AP is due to a

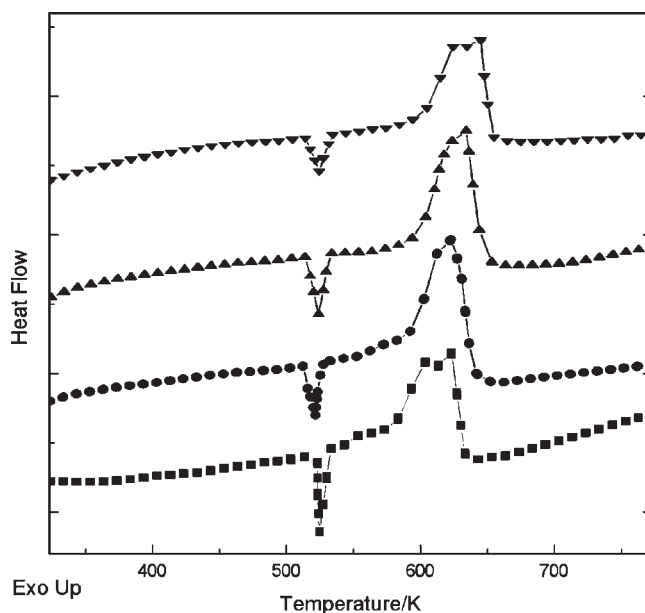


**Figure 6.** DSC curves of AP with additives at various heating rates: ■,  $\beta = 5 \text{ K} \cdot \text{min}^{-1}$ ; ●,  $\beta = 10 \text{ K} \cdot \text{min}^{-1}$ ; ▲,  $\beta = 15 \text{ K} \cdot \text{min}^{-1}$ ; ▼,  $\beta = 20 \text{ K} \cdot \text{min}^{-1}$ .

crystallographic transition of AP from the orthorhombic to cubic phase. The second and third peaks for pure AP are exothermic, which correspond to the low-temperature decomposition (LTD) process and high-temperature decomposition (HTD) process.<sup>20</sup> The exothermic peak of the LTD process at about 563 K with the heating rate of  $10 \text{ K} \cdot \text{min}^{-1}$  corresponds to the decomposition of AP with the heat of  $0.735 \text{ kJ} \cdot \text{g}^{-1}$ , while the exothermic peak for HTD process is at 715 K with the heat of  $0.787 \text{ kJ} \cdot \text{g}^{-1}$ .

Complex 1 and AP were mixed at a mass ratio of 1:3 to prepare the target sample for thermal decomposition analyses. The sample has no effect on the crystallographic transition temperature, and the exothermic peak occurring at 628 K changes into a sharp one. The onsets of thermal decomposition for pure AP and the mixture are all under 573 K, while the end temperatures are about (763 and 658) K, respectively. AP is completely decomposed in a shorter time in the presence of the complex. Moreover, the decomposition heat of the mixture is  $2.034 \text{ kJ} \cdot \text{g}^{-1}$ , significantly higher than pure AP.

It is known that the decomposition temperature is related to the heating rate. The relationship between decomposition temperature and heating rate can be described by the Kissinger correlation.

$$\ln \frac{\beta}{T_p^2} = \ln \frac{AR}{E_a} - \frac{E_a}{RT_p}$$

where  $E_a$  is the apparent activation energy,  $\beta$  is the heating rate,  $R$  is the gas constant,  $T_p$  is the peak temperature, and  $A$  is the pre-exponential factor. According to this equation, the values of activation  $E_a$  are obtained by Kissinger's method at four different heating rates (Figure 6). As shown in Table 3, the activation energy of pure AP is  $74.65 \text{ kJ} \cdot \text{mol}^{-1}$ . With the presence of 1, the activation energy is changed to  $206.11 \text{ kJ} \cdot \text{mol}^{-1}$ . The activation energy of AP decomposition is not a parameter that describes the decomposition process, and the increased activation energy is caused by the kinetic compensation effect.<sup>21</sup> The value of pre-exponential factor  $A$  should be considered, and the ratio of  $E_a/\ln(A)$  could be used to describe

**Table 3. Kinetic Parameters of Thermal Decomposition for AP and AP with Additives ( $T_p$  and  $\Delta H$  Were Given at the Heating Rate of  $10\text{ K}\cdot\text{min}^{-1}$ )**

	$T_p$	$\Delta H$	$E_a$			$r$
	K	$\text{kJ}\cdot\text{g}^{-1}$	$\text{kJ}\cdot\text{mol}^{-1}$	$\ln[A/s]$	$E_a/\ln A$	
AP	563	0.735	74.65	5.71	14.21	0.9830
1 + AP	628	2.034	206.11	16.28	12.66	0.9907

the reactivity.<sup>22,23</sup> Usually, a bigger ratio means a greater stability of the reactant.<sup>21</sup> The ratios of  $E_a/\ln(A)$  are 14.1 for pure AP and 12.66 for the mixture. The title complex shows good catalytic activity toward AP decomposition, which indicates the potential application in solid propellants.

## CONCLUSIONS

In summary, the title complex has been successfully synthesized, and the structure was determined by single crystal X-ray diffraction. Each Co(III) was six-coordinated with three 2,3'-bpt in a distorted octahedral geometry. The DSC experiment revealed that the complex accelerated the thermal decomposition of AP. The present study projects the probable application of the title complex in a solid propellant field.

## ASSOCIATED CONTENT

**S Supporting Information.** CCDC 807006 (cif file) with supplementary crystallographic data for this paper. This material is available free of charge via the Internet at <http://pubs.acs.org>. These data can also be obtained free of charge at <http://www.ccdc.ac.uk/conts/retrieving.html> or from the Cambridge Crystallographic Data Center (CCDC), 12 Union Road, Cambridge CB21EZ, UK; fax: +44 1223 336033; e-mail: [deposit@ccdc.cam.ac.uk](mailto:deposit@ccdc.cam.ac.uk).

## AUTHOR INFORMATION

### Corresponding Author

\*E-mail address: [sanpingchen@126.com](mailto:sanpingchen@126.com) (S.-P. Chen), [gaoshli@nwu.edu.cn](mailto:gaoshli@nwu.edu.cn) (S.-L. Gao).

### Funding Sources

We gratefully acknowledge the financial support from the National Natural Science Foundation of China (Grant No. 20873100) and the National Natural Science Foundation of Education Department of Shaanxi Province (No. 09JS089, 2010JQ2007, and 2010JK882).

## REFERENCES

- Jacobs, P. W. M.; Whitehead, H. M. Decomposition and combustion of ammonium perchlorate. *Chem. Rev.* **1969**, *69*, 551–590.
- Boldyrev, V. V. Thermal decomposition of ammonium perchlorate. *Thermochim. Acta* **2006**, *443*, 1–36.
- Wang, Y. P.; Zhu, J. W.; Yang, X. J.; Lu, L.; Wang, X. Preparation of NiO nanoparticles and their catalytic activity in the thermal decomposition of ammonium perchlorate. *Thermochim. Acta* **2005**, *437*, 106–109.
- Chen, L. J.; Li, L. P.; Li, G. S. Synthesis of CuO nanorods and their catalytic activity in the thermal decomposition of ammonium perchlorate. *J. Alloys Compd.* **2008**, *464*, 532–536.
- Cui, P.; Feng, S. L.; Zhou, J.; Jiang, W. Preparation of Cu/CNT Composite Particles and Catalytic Performance on Thermal Decomposition of Ammonium Perchlorate. *Propellants, Explos., Pyrotech.* **2006**, *31*, 452–455.

(6) Singh, G.; Prem Felix, S. Studies on energetic compounds: 25. An overview of preparation, thermolysis and applications of the salts of 5-nitro-2,4-dihydro-3H-1,2,4-triazol-3-one (NTO). *J. Hazard. Mater.* **2002**, *90*, 1–17.

(7) Kulkarni, P. B.; Reddy, T. S.; Nair, J. K.; Nazare, A. N.; Talawar, M. B.; Mukundan, T.; Asthana, S. N. Studies on salts of 3-nitro-1,2,4-triazol-5-one (NTO) and 2,4,6-trinitroanilino benzoic acid (TABA): Potential energetic ballistic modifiers. *J. Hazard. Mater.* **2005**, *123*, 54–60.

(8) Zhang, J. P.; Lin, Y. Y.; Huang, X. C.; Chen, X. M. Copper(I) 1,2,4-triazolates and related complexes: Studies of the solvothermal ligand reactions, network topologies, and photoluminescence properties. *J. Am. Chem. Soc.* **2005**, *127*, 5495–5506.

(9) Huang, F. P.; Tian, J. L.; Gu, W.; Liu, X.; Yan, S. P.; Liao, D. Z.; Cheng, P. Co(II) Coordination Polymers: Positional Isomeric Effect, Structural and Magnetic Diversification. *Cryst. Growth. Des.* **2010**, *10*, 1145–1154.

(10) Du, M.; Zhang, Z. H.; You, Y. P.; Zhao, X. J. R-Isophthalate (R = -H, -NO<sub>2</sub>, and -COOH) as modular building blocks for mixed-ligand coordination polymers incorporated with a versatile connector 4-amino-3,5-bis(3-pyridyl)-1,2,4-triazole. *Cryst. Eng. Commun.* **2008**, *10*, 306–321.

(11) Xie, X. F.; Chen, S. P.; Xia, Z. Q.; Gao, S. L. Construction of metal-organic frameworks with transitional metals based on the 3,5-bis(4-pyridyl)-1H-1,2,4-triazole ligand. *Polyhedron* **2009**, *28*, 679–688.

(12) Huang, F. P.; Tian, J. L.; Gu, W.; Yan, S. P. Three 3D Cu(II) coordination polymers constructed from 1,2,4,5-benzenetetracarboxylate acid and three positional isomeric ligands. *Inorg. Chem. Commun.* **2010**, *13*, 90–94.

(13) Li, B.; Chen, S. P.; Yang, Q.; Gao, S. L. R-phenyldicarboxylate (R = H, NO<sub>2</sub>, and COOH) modular effect on Ni(II) coordination polymers incorporated with a versatile connector 1H-3-(3-pyridyl)-5-(4-pyridyl)-1,2,4-triazole. *Polyhedron* **2011**, *30*, 1213–1218.

(14) Singh, G.; Felix, S. P. Studies of energetic compounds, part 29: effect of NTO and its salts on the combustion and condensed phase thermolysis of composite solid propellants, HTPB-AP. *Combust. Flame* **2003**, *132*, 422–432.

(15) Sheldrick, G. M. *SHELXS 97*, Program for the Solution of Crystal Structure; University of Göttingen: Göttingen, Germany, 1997.

(16) Sheldrick, G. M. *SHELXL 97*, Program for the Refinement of Crystal Structure; University of Göttingen: Göttingen, Germany, 1997.

(17) Browne, E. 1,2,4-Triazol-3-ylpyridines. *Aust. J. Chem.* **1975**, *28*, 2543–2546.

(18) Wang, J. P.; Ma, P. T.; Shen, Y.; Niu, J. Y. Tetra-Transition-Metal Substituted Weakley-Type Sandwich Germanotungstates and their Derivatives Decorated by Transition-Metal Complexes. *Cryst. Growth Des.* **2008**, *8*, 3130–3133.

(19) Li, Q. Y.; Fu, Y. L. A layered iodocuprate based on a 3D cationic supramolecular network of dimeric Co(II) complexes by offset face-to-face interactions. *Cryst. Eng. Commun.* **2009**, *11*, 1515–1518.

(20) Vyazovkin, S.; Wight, C. A. Kinetics of Thermal Decomposition of Cubic Ammonium Perchlorate. *Chem. Mater.* **1999**, *11*, 3386–3393.

(21) Li, L. P.; Sun, X. F.; Qiu, X. Q.; Xu, J. X.; Li, G. S. Nature of Catalytic Activities of CoO Nanocrystals in Thermal Decomposition of Ammonium Perchlorate. *Inorg. Chem.* **2008**, *47*, 8839–8846.

(22) Brill, T. B.; Gongwer, P. E.; Williams, G. K. Thermal Decomposition of Energetic Materials. 66. Kinetic Compensation Effects in HMX, RDX, and NTO. *J. Phys. Chem.* **1994**, *98*, 12242–12247.

(23) Andričić, B.; Kovacic, T.; Klarić, I. Kinetic analysis of the thermooxidative degradation of poly(vinyl-chloride) in poly(vinyl chloride)/methyl methacrylate-butadiene-styrene blends 2. Nonisothermal degradation. *Polym. Degrad. Stab.* **2003**, *79*, 265–270.